



**HAL**  
open science

## Influence of the CNC behaviour on the laser spot trajectory in LPBF process

Kevin Godineau, Sylvain Lavernhe, Christophe Tournier

► **To cite this version:**

Kevin Godineau, Sylvain Lavernhe, Christophe Tournier. Influence of the CNC behaviour on the laser spot trajectory in LPBF process. Joint Special Interest Group meeting between euspen and ASPE Advancing Precision in Additive Manufacturing, Sep 2021, St Gallen, Switzerland. hal-03372979

**HAL Id: hal-03372979**

**<https://hal.science/hal-03372979>**

Submitted on 11 Oct 2021

**HAL** is a multi-disciplinary open access archive for the deposit and dissemination of scientific research documents, whether they are published or not. The documents may come from teaching and research institutions in France or abroad, or from public or private research centers.

L'archive ouverte pluridisciplinaire **HAL**, est destinée au dépôt et à la diffusion de documents scientifiques de niveau recherche, publiés ou non, émanant des établissements d'enseignement et de recherche français ou étrangers, des laboratoires publics ou privés.

## Influence of the CNC behaviour on the laser spot trajectory in LPBF process

Kevin. Godineau<sup>1</sup>, Sylvain. Lavernhe<sup>1</sup>, Christophe. Tournier<sup>1</sup>

<sup>1</sup>Université Paris-Saclay, ENS Paris-Saclay, Institut Farman FR3311, LURPA, France

[kevin.godineau@ens-paris-saclay.fr](mailto:kevin.godineau@ens-paris-saclay.fr)

### Abstract

The quality of the parts produced in additive manufacturing by laser powder bed fusion (LPBF) depends on the understanding of all the physics involved in the process. In LPBF, the effective path of the laser spot is rarely studied and existing works are mainly focused on the choice of the scanning strategy and its parameters. However, the programmed scanning path during the CAM stage is adapted by the numerical control (NC) unit of the manufacturing machine in order to generate admissible setpoints for the actuators (galvanometers). This modification locally generates deviations on the scanning path and significant decrease of the laser spot velocity. In order to identify the NC unit behaviour, a test bench that replicates an industrial machine has been developed. This test bench allows the acquisition of the setpoints sent to the actuators and their real positions at a frequency of 100 kHz, as well as the energy deposited by the laser spot in the work plane. An analysis of those data shows that the processing done by the NC is based on a filtering method which in some cases can generate a deviation of the scanning path of more than 100  $\mu\text{m}$  for a programmed speed of 2 m/s. Finally, in order to correctly estimate the amount of energy brought by the laser on the powder, a dedicated model has been developed. This model takes into account the dynamics of the actuators, the behaviour of the NC unit and the optical chain of the system. Experimental tests have been conducted to validate the simulations produced by the proposed model.

Accuracy, Computer numerical control (CNC), Identification, Monitoring

### 1. Introduction

The control of the effective path of the laser spot plays an essential role in LPBF process. Indeed, the movement of the laser spot on the powder bed allows distributing the energy necessary for the fusion. The work described in this paper highlights the impact of the numerical control unit behaviour on the effective path of the laser spot. The numerical control unit performs the following operations (also shown in figure 1):

1. Sampling - interpolate the paths generated by the slicer  $X^{cons}$  into a set of laser spot positions  $X^{inter}$ .
2. Inverse Kinematic Transformation (IKT) - convert laser spot positions  $X^{inter}$  into actuator positions  $Q^{inter}$ .
3. Geometric and Time Interpolation - locally modify the positions  $Q^{inter}$  to produce setpoints  $Q^{filt2}$  that respect the kinematic constraints of the actuators.

Step 3 is required because the paths generated by the slicer are not physically achievable, as they assume infinite accelerations of the actuators.

These 3 steps generate local modifications of the velocity and the effective path. This aspect is never taken into account in thermal simulations and is nevertheless critical, as it leads to greater energy deposition locally on the part. In machining and robotics, the operations carried out by the numerical control unit are well known and are the subject of many works. Those works are focused on the optimization of the instructions sent to the actuators to control the effective path of the system with respect to the kinematic constraints of the actuators [1].

In LPBF additive manufacturing, very few works deal with time interpolation of laser spot path. Wienken et al highlight the

developments of the SCANLAB company and succinctly describe the operation of the actuator control structure [2]. Trajectories that are initially speed-limited are processed to be transformed into acceleration-limited trajectories.

A research team at the National Institute of Standards and Technology (NIST) is also working on these aspects. For this purpose, they have developed a replica of a LPBF additive manufacturing machine [3]. Using this platform, they are able to analyse the control laws used by the industrial controller (velocity-limited laws) and implemented acceleration-limited [4] and jerk-limited [5] motion laws. The integration of these laws makes it possible to obtain setpoints that are less demanding on the actuators and are therefore better respected by the system.

The work carried out in this paper concerns the study and characterization of an existing industrial CNC. The analysis of this system allows us to highlight its limits and thus to underline the possible improvements.

This paper is organized as follows: section 2 is dedicated to the design of the test bench. The analysis of the different signals allows in section 3 to identify the behaviour of the CNC system and its impact on the effective path. This knowledge is used to set up a simulator of the energy supplied to the powder bed. This model is briefly presented and experimentally validated in section 4 before concluding remarks.

### 2. Design of the test bench

In this section, the developed test bench is presented and different signals are analysed to identify the control solutions implemented in the industrial numerical controller.

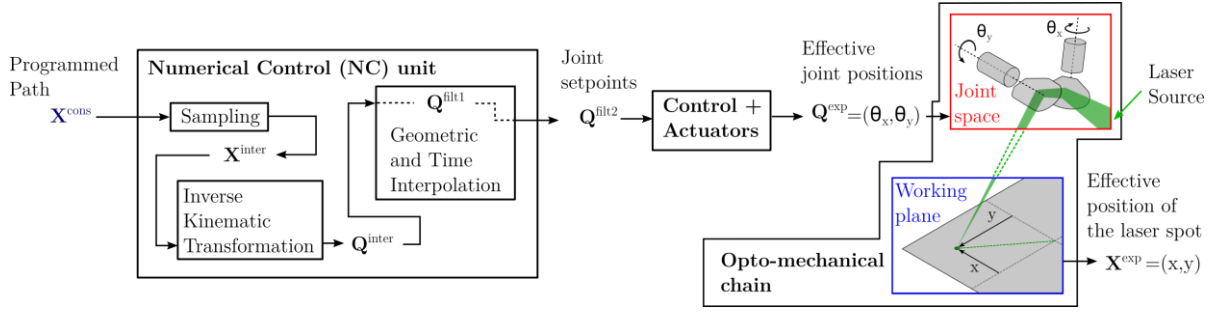


Figure 1. Architecture of the industrial numerical controller and the test bench developed.

### 2.1. Description of the test bench architecture

The architecture of the developed platform is shown in Figure 1. This platform integrates an industrial chain currently used in several LPBF additive manufacturing machines. The different signals used in this paper are presented in Figure 1. Signals that have not already been described are explained in the following list:

- $Q^{filt1}$  refers to the internal setpoints of the time and geometry interpolation step.
- $Q^{filt2}$  represents the joint position setpoints sent to the control system.
- $Q^{exp}$  and  $X^{exp}$  represent respectively the joint positions of the actuators and the real positions of the laser spot in the working plane.

The test bench is completed with a camera in order to measure the energy deposited on the surface of the working plane. To simplify the measurements and minimize sources of error, the laser beam is fired directly on to the CCD matrix. This allows the trace of the laser spot to be observed. The technological solution used is detailed in [6].

### 2.2. Data analysis

To better understand the operations performed in the CNC, the joint signals  $Q^{inter}$ ,  $Q^{filt1}$  and  $Q^{filt2}$  are derived to observe the angular velocities as well as the angular accelerations.

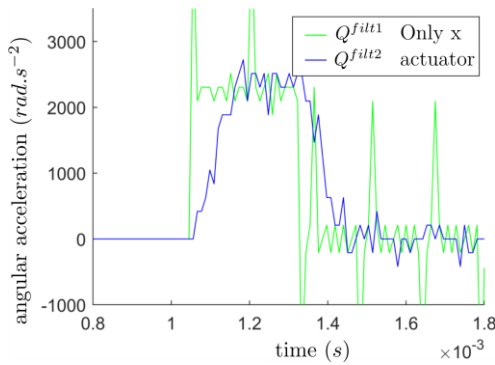


Figure 2. Angular acceleration measurement of the actuator  $x$ .

Figure 2 shows the angular accelerations of the different signals. For readability consideration, the signal  $Q^{inter}$  and  $Q^{exp}$  are not displayed. The input setpoints correspond to a velocity jump of the  $x$ -axis. The signal  $Q^{filt1}$  represents an acceleration pulse of duration  $T_1 = 260 \mu s$ . The signal  $Q^{filt2}$  represents an acceleration trapezoid whose rising and falling phase duration is identical and equal to  $T_2 = 125 \mu s$ . The  $Q^{filt2}$  signal therefore corresponds to a jerk-limited signal (acceleration trapezoid).

Observations made on this test were repeated for other setpoints on both actuators. The conclusions on the duration of the jerk and acceleration phases are identical. The same applies to the deceleration phases. The study of the literature shows

that the processing carried out by the numerical control unit is based on a finite impulse response (FIR) gate filtering approach [7]. The solution used consists of two successive gate filters of characteristic times  $T_1$  and  $T_2$ . These two filters of fixed duration make it possible to limit the maximum acceleration and jerk.

A velocity saturation is also performed between  $Q^{filt1}$  and  $Q^{filt2}$  when the setpoint exceeds the maximum velocity value of  $25 \text{ rad.s}^{-1}$ . In this work, such angular velocities are never requested from the actuators. Indeed, to request a single actuator (galvanometer) for this angular velocity would be tantamount to requesting for a laser spot velocity in the work plane of approximately  $35 \text{ m.s}^{-1}$ .

### 3. Analysis of the NC behaviour

In this section the influence of filtering on the velocity and the contour error is highlighted. An analysis of the system dynamics is also performed. Finally, all these developments are experimentally validated.

#### 3.1. Assumptions and parameterization

To simplify the understanding, we will consider in the following work that the filters are applied on the  $X^{inter}$  setpoints in the working plane. The impact of the inverse kinematic transformation (IKT) on the filtering operation is therefore considered negligible. This assumption is validated through simulations. Over the whole angular range of the actuators and for velocity lower than  $10 \text{ m.s}^{-1}$  this assumption generates deviations that do not exceed  $10^{-8} \text{ rad}$ . This error transcribed on the working plane is therefore negligible because less than  $0.1 \mu m$ .

Finally, to simplify the study we are interested in the realization of a path composed of two successive segments represented in Figure 3. The programmed path is shown in black and the filtered one in blue.

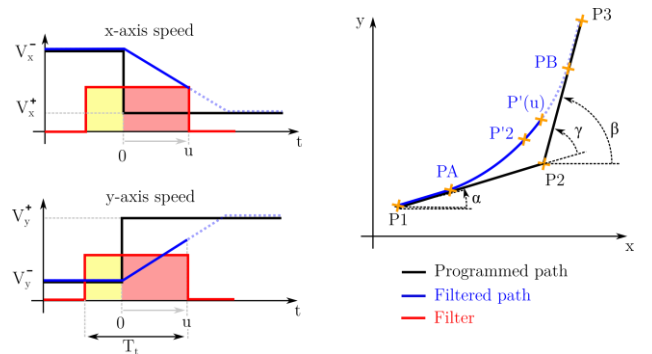


Figure 3. Parameterization of a filtering operation. Example with a gate filter.

1. The programmed velocity of the path is called  $V_{eff}$ .

2. The velocity of the x-axis is noted  $V_x^-$  on the segment  $(P1, P2)$  and  $V_x^+$  on  $(P2, P3)$  (same for y-axis).
3. The oriented angle between the two segments is noted  $\gamma$
4. The interaction time between the filter and the second segment of the path is noted  $u$ .
5. The function  $a(u)$  corresponds to the algebraic area of the filter during the time  $u$  (red area on Figure 3).
6. The time of the filter, noted  $T_t$ , is symmetric and has a unit area  $a(T_t) = 1$ .
7. The function  $A(u)$  corresponds to the integral of the algebraic area of the filter during time  $u$ .
8. When  $u = 0$  the filter has no impact on the geometry of the path. The current point  $P'(u)$  is located in  $PA$ .
9. When  $u = T_t$  the filter has no longer impact on the path. The current point  $P'(u)$  is located in  $PB$ .

### 3.2. Influence of filtering on path velocity

Firstly, the velocity of the filtered path is studied. The knowledge of this velocity is important, because a decrease of it leads to an increase of the deposited energy if the laser power is constant. The velocity of the x-axis is expressed in equation (1) (same for the y-axis).

$$Vf_x(u) = (1 - a(u))V_x^- + a(u)V_x^+ \quad (1)$$

The norm of the velocities  $Vf_x(u)$  and  $Vf_y(u)$  is used to calculate the tangential velocity of the filtered path. This velocity is written in equation (2).

$$Vf(u) = V_{eff} \sqrt{1 + 2 \cdot a(u)(1 - a(u))(\cos(\gamma) - 1)} \quad (2)$$

For a symmetric filter of unit area, the minimum of this function is obtained in  $u = T_t/2$ . The minimum velocity of the filtered path is expressed in equation (3).

$$Vf\left(u = \frac{T_t}{2}\right) = Vf_{min} = V_{eff} \left| \cos\left(\frac{\gamma}{2}\right) \right| \quad (3)$$

As shown in equation (3) the minimum velocity of the filtered path is independent of the filter used. This minimum velocity depends only on the tangential velocity and the angle between the two consecutive segments.  $Vf_{min} = V_{eff}$  for  $\gamma = 0$  and  $Vf_{min} = 0$  for  $\gamma = 180 \text{ deg}$ . This equation is verified experimentally in section 3.5.

### 3.3. Influence of filtering on the contour error

It is also important to study the geometry of the filtered path. Indeed, this geometry has an impact on the effective path and therefore on the geometry of the built part. To study this, the contour deviation criterion  $e_c$  is used. This criterion defines for each point of the theoretical path the minimum distance between the whole filtered path and this point.

The filtered path  $P'(u)$  shown in Figure 3 is calculated by starting from the position of the point  $PA$  and integrating the filtered velocity obtained in equation (1). After simplification, the equation (4) is obtained which gives the distance between the filtered path  $P'(u)$  and the point  $P2$ .

$$\|P'(u) - P2\| = V_{eff} \left[ \left(u - \frac{T_t}{2}\right)^2 + 2A(u) \left(u - \frac{T_t}{2} - A(u)\right) (\cos(\gamma) - 1) \right]^{1/2} \quad (4)$$

If the filter is positive then the functions  $a(u)$  and  $A(u)$  are monotone (increasing) and positive. Under this condition, the maximum contour deviation is obtained in  $u = T_t/2$ . The

contour deviation then corresponds to the distance between  $P'2$  and  $P2$ . The point  $P'2$  is then located on the bisector between the two consecutive segments. The previous equation can thus be simplified to obtain equation (5).

$$e_c = 2 \cdot V_{eff} A\left(\frac{T_t}{2}\right) \left| \sin\left(\frac{\gamma}{2}\right) \right| \quad (5)$$

This equation describes the deviation from the contour as a function of the integral of the filter area, the velocity of the programmed path and the oriented angle between the two consecutive segments. This equation is valid for all positive symmetric filters of unit area.

When applying equation (5) to a trapezoidal filter (combination of two gate filters of durations  $T_1$  and  $T_2$  with  $T_1 > T_2$ ) equation (5) becomes:

$$e_c = V_{eff} \frac{T_2^2 + 3T_1^2}{12T_1} \left| \sin\left(\frac{\gamma}{2}\right) \right| \quad (6)$$

Equation (6) is verified experimentally in section 3.5.

### 3.4. Identification of the dynamic behaviour of the system

Now that the architecture is known, it is possible to identify the dynamic behaviour of the control system and the actuators. To do this, sinusoidal setpoints are sent to each axis.

Figure 4 shows the ratio between the amplitudes of  $Q^{exp}$  and  $Q^{filter}$  signals at different frequencies. This figure shows the behaviour of the actuators and their control structures. The assembly associated with the y actuator is less dynamic, this is due to the fact that the mirror has a greater inertia.

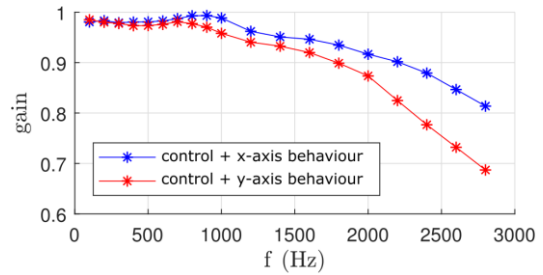


Figure 4. Bode diagram of the behaviour of the assembly (Control + Galvanometer).

### 3.5. Experimental validation

In order to confirm the developments made in sections 3.3 and 3.4, several paths with different velocity and angles were performed. Figure 5(a) shows the set path, the filtered path and the actual path. Figures 5(b) and 5(c) show respectively the tangential velocity and contour error profiles

For angle 1 ( $\gamma = 53,13 \text{ deg}$ ) equations (3) and (6) predict a minimum velocity of  $1789 \text{ m} \cdot \text{s}^{-1}$  and a contour error of  $62 \mu\text{m}$ . The experimental results show that the minimum velocity of the filtered set points is  $1708 \text{ m} \cdot \text{s}^{-1}$  and the contour error is  $62 \mu\text{m}$ . For angle 2 ( $\gamma = 108,43 \text{ deg}$ ) the theoretical velocity is  $1170 \text{ m} \cdot \text{s}^{-1}$  and the contour error is  $114 \mu\text{m}$ . The measurements show a minimum velocity of  $1101 \text{ m} \cdot \text{s}^{-1}$  and a contour error of  $109 \mu\text{m}$ . The deviations between theory and measurement in velocity are mostly due to errors in sampling of the setpoints made in the numerical control unit.

The effective path is very similar to the filtered path. This is due to the actuator servo control, which is very efficient, and to the filtering, which allows the generation of achievable setpoints.

By studying the filtering further, the limits of the employed solution can be shown. For example, the acceleration and deceleration duration is always constant, regardless of the value of the requested velocity. The actuators are therefore not used to their full capabilities. It is thus possible to improve this solution by adapting the filter duration to the solicitation. This would save time without necessarily losing quality.

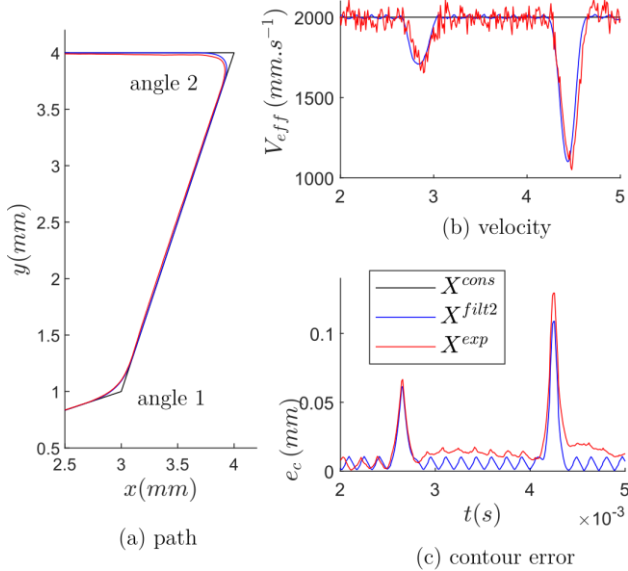


Figure 5. Path performed at a programmed velocity  $V_{eff} = 2 \text{ m.s}^{-1}$ .

#### 4. Impact on the energy provided to the powder

Now that the impact of the system dynamics on the path has been quantified, it remains to add the energetic behaviour of the laser source in order to establish a model in order to simulate the energy deposition on the powder bed.

The modelling of the laser source and the measurement protocol of the deposited energy are described in [6]. The developed simulator takes into account:

1. the behaviour of the CNC identified in section 2.2, 3.2 and 3.3;
2. the dynamics of the actuators as well as the servo control identified in section 3.4;
3. the energy distribution of the laser source which is in this paper considered as Gaussian;
4. the influence of the opto-mechanical chain on the energy delivered by the laser spot on the powder bed [6].

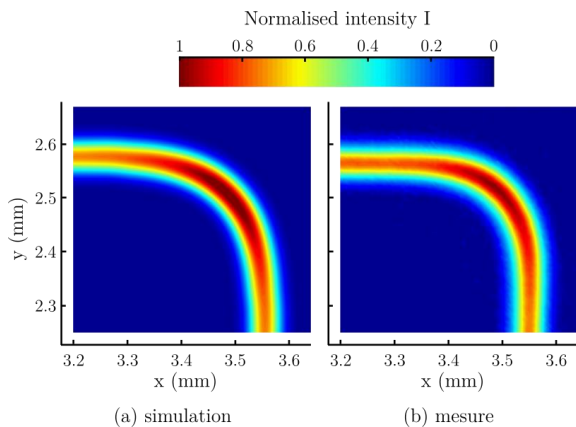


Figure 6. Influence of interpolation on a path composed of two right-angled segments for a programmed velocity  $V_{eff} = 1,5 \text{ m.s}^{-1}$ .

Figure 6 shows the energy delivered to the powder bed in the case of a right-angle path of programmed velocity  $V_{eff} = 1,5 \text{ m.s}^{-1}$ . The laser beam used on the test bench is of very low power ( $1 \text{ mW}$ ) in order not to damage the CCD matrix. Thus, for readability purposes, the intensity is normalised.

The geometrical deviations from the target path are in good agreement with equation (6). The decrease in velocity observed in the corner generates an accumulation of energy. The simulator is accurate and allows the energy provided to the material to be quantified. The deviations on the maximum amplitude are about 5% and the differences between the model and the measurement are mainly due to the energy distribution of the laser source at the entrance of the opto-mechanical chain. The experimental energy distribution of the laser source is not perfectly a gaussian distribution which is an assumption made here.

#### 5. Conclusion and perspectives

A test bench has been developed in order to study the impact of the CNC processing on the laser spot path. Filtering solutions have been highlighted. These solutions lead to velocity decreases as well as significant deviations from the CAM path. The identification of the machine's behaviour has allowed the development of a simulator to study the energy provided to the powder bed.

This work can greatly improve thermal simulations by taking into account the effective path and tangential velocity of the laser spot. This study also highlights numerous perspectives related to the development of new control strategies. For example, it seems relevant to couple the power of the laser beam and the kinematics of the trajectories in order to homogenize the energy deposition.

#### Acknowledgements

This work is supported by the SOFIA project and funded by Bpifrance.

#### References

- [1] Tajima S, Sencer B and Shamoto E, "Accurate interpolation of machining tool-paths based on FIR filtering" *Precision Engineering*, vol. **52**, pp. 332-344, 2018
- [2] Wienken C. J., Unterholzner A and Breit M, "Advanced galvo control enables efficient laser micro processing" *9th International Conference on Photonic Technologies*, LANE 2016
- [3] Lane B and al., "Design, Developments, and Results from the NIST Additive Manufacturing Metrology Testbed (AMMT)" *Proceedings of the 26th Annual International Solid Freeform Fabrication Symposium--An Additive Manufacturing Conference*, pp. 1145-1160, 2016
- [4] Yeung H, Neira J, Lane B, Fox J and Lopez F, "Laser Path Planning and Power Control Strategies for Powder Bed Fusion Systems" *Solid Freeform Fabrication Symposium*, 2016
- [5] Yeung H, Lane B, Donmez M, Fox J and Neira J, "Implementation of Advanced Laser Control Strategies for Powder Bed Fusion Systems" *Procedia Manufacturing*, vol. **26**, pp. 871-879, 2018
- [6] Godineau K, Lavernhe S and Tournier C, "Influence of the opto-mechanical chain on the energy provided by the laser spot to the material in laser powder bed fusion processes" *EUSPEN Special Interest Group Meeting*, 2019
- [7] Biagiotti L and Melchiorri C, "FIR filters for online trajectory planning with time-and frequency-domain specifications" *Control Engineering Practice*, vol. **20**, pp. 1385-1399, 2012